Call: ELI-RO 2020 **Project acronym: PHARDIPLAS**

ELI-NP Thematics:

LGE/IV.1 Laser-plasma interaction - experiments, simulations

LGE/IV.3 Plasma diagnostics for ELI-NP laser experiments

LGE/III.2 Evaluation of High Energy Ionizing Radiation Effects in Materials

Midterm Summary Document

Year: Oct. 2020 - Jun. 2022

Project Title: Plasma harmonics for diagnosing plasma and driving laser/ PHARDIPLAS

Project Work Plan (according to the contract)

Stage: I - 2020

Activities:

I.1. Study of the plasma mirror model for HHG and plasma dynamics, numerical programming in COMSOL and MATLAB.

I.2. Project management.

Stage: II- 2021

Activities:

II.1. Numerical simulations on HHG and plasma dynamics.

II.2. Experiments on efficiency of HHG on solid and gas targets.

II.3. Project management and dissemination of results

Stage: III - 2022

Activities:

III.1. Experimental study on properties of harmonics in relation to properties of driving laser in focus for laser diagnosis

III.2. Determination of main characteristics of optical fibres used near the target when exposed to UV, X and gamma radiation (on going)

III.3. Project management and disemination of results (on going)

1. Cover Page

- Specific scientific focus of group (state physics of subfield of focus and group's role);

The scientific focus of the group was related to the: numerical simulation (in COMSOL and MATLAB) of the harmonic generation process; laser-matter interaction with focus on non-linear optics in laser produced plasmas; determination of main characteristics of optical fibers used near the target when exposed to gamma radiation at different doses.

- Summary of accomplishments during the reporting period.

The members of the group succeeded in the following activities related to the project objectives:
- developed scripts in COMSOL and MATLAB for 2D calculation of the properties of the harmonics (third, fifth, etc) generated in gas plasmas as a function of pump laser properties.
- developed script in MATLAB to evaluate numerically the momentum transferred by high power laser on solid targets in single and multi-pulse regime in connection to the plasma produced at the target surface.
- analyzed experimentally the properties of third harmonic radiation (i.e. intensity, time and space distribution) as a function of pump-laser properties: intensity, polarization
- published two ISI papers:

i. one Q2 paper on harmonics generation in an American journal:

M. Stafe, "Three-step model for third-harmonic generation in air by nanosecond lasers", JOURNAL OF THE OPTICAL SOCIETY OF AMERICA B-OPTICAL PHYSICS 38 (7), 2206-2214 (2021)

ii. one paper on optimum conditions for third harmonic generation in an ISI journal:

Mihai STAFE, Constantin NEGUȚU, Georgiana C. VASILE, and Niculae N. PUȘCAȘ, "Theoretical and experimental study ongeometry related phase-matching condition for third harmonic generation", U.P.B. Sci. Bull., Series A, Vol. 84, Iss. 2, 163-174 (2022)

- submitted one paper for the Proceedings of an international conference (ATOM-N2022) to be held on August 2022. Paper title: *Third harmonics emission with nanosecond and femtosecond lasers in air. Gamma radiation effects on optical fibers,* Authors: Mihai Stafe, Georgiana C. Vasile, Răzvan Mihalcea, Constantin Daniel Neguț, Constantin Neguțu, Niculae N. Pușcaș.

2. Scientific accomplishments – Results obtained during the reporting period.

Result 1. Numerical simulations on HHG and plasma dynamics with COMSOL/ MATLAB

In the last years several authors investigated extensively the phase matching limitations associated with focal geometry in the process of harmonics generation. Typically, a particular generated harmonic and the fundamental laser field are matched in phase over distances that are many times the wavelength of the incident light. However, the length over which the harmonic phases are matched (i.e.the coherence length) can be much shorter than the focal depth (typically, 1 mm) owing to different rates of diffraction for different wavelengths. Because of these issues, it is typical to confine the interaction region in the non-linear (NL) medium to a single geometrical coherence length to avoid destructive phase cancellations. This is usually done by lengthening the laser focus relative to the width of the NL medium by working outside of the focus. As mentioned above, this method does not utilize the high-intensity focal volume outside of the coherence length. After a coherence length, new harmonic production is out of phase with previously generated harmonic light (Fig. 1) The generation of a particular harmonic can go in and out of phase many times in the laser focus. Harmonic light generated at the first position is out of phase with the harmonic light generated at the second position, but in phase with the light generated at the third position.

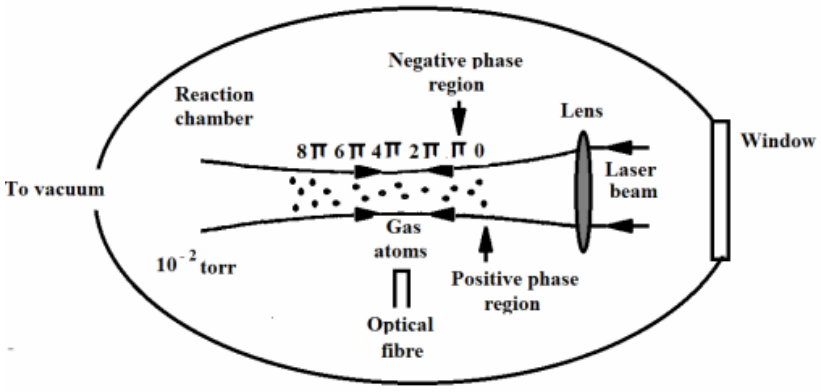

Fig. 1. Phase variation of harmonic emission throughout the laser focus.

The generation of third, fifth, … *q*-th harmonic in a homogenous gas plasma is described by the NL polarization oscillating at q-th frequency:

$$P_{NL\,y}(\omega_q = q\omega) = \varepsilon_0 \chi^{(q)} \left(E_{\omega y}\right)^q . \qquad (1)$$

The coupled wave equations describing the propagation of the fundamental (F, q=1) and third harmonic (TH, q=3) radiations within the NL medium can be written vectorially in a concise way as follows:

$$\nabla \times (\nabla \times \boldsymbol{E}_q) - k_q^2 \left(\varepsilon_{rq} - \frac{i\sigma_q}{\omega_q \varepsilon_0}\right) \boldsymbol{E}_q = \omega_q^2 \mu_0 \boldsymbol{P}_{NL}(\omega_q) \quad (2)$$

Here, ε_{rq} denotes the frequency dependent dielectric constant of the NL medium due to neutral molecules, describing the positive dispersion of the medium: ε_{r1} = 1.00055 and ε_{r3} = 1.00057.σ_q is the frequency dependent plasma conductivity, the imaginary part of σ_q describing the anomalous negative dispersion.σ_q is directly related to the free electron density, and thereby to the nitrogen ions density N_i. The third order susceptibility $\chi^{(3)}$ is also directly related to the density N_i.

We used Newton method implemented in COMSOL software to solve numerically the coupled Eqs. (2) in the frequency domain. For time-dependent case, we use an accurate time-dependent solver with implicit time stepping method: generalized alpha method which contains a parameter, called alpha in the literature, to control the degree of damping of high frequencies. The output data of the COMSOL are stored in Excel worksheets. These worksheets act both as data storage and as feed-in for a successive program in MATLAB that processes these data to calculate additional characteristic measures of the non-linear process.

Due to the symmetry of the problem, we chose a 2D rectangular domain with the *x* axis corresponding to the propagation direction of the radiation, and *y* to the polarization direction. The origin of the *x* axis is in the focal plane and the origin of *y* axis is in the center of the F gaussian beam. The dimensions of the rectangular domain are $4x_0$ in the axial *x* direction and $8w_0$ in the transverse *y* direction. Here, x_0 is the Rayleigh length and w_0 denotes the beam waist. In 2D geometry, the Gaussian profile of the F pulse impinging on the front boundary positioned at $x = -2x_0$ is defined as

$$E_{1y,inc} = E_0 \sqrt{\frac{w_0}{w}} \exp\left(-\frac{w^2}{2w_0^2}\right) \exp\left[-i\left(k_1 x + k_1 \frac{y^2}{R} - \eta\right)\right], \quad (3)$$

whereas there is no incident field at TH frequency on the front boundary: $E_{3y,inc} = 0$. Here, E_0 is the field amplitude, $w(x)$ denotes the beam radius at axial *x* position, $R(x)$is the position dependent wavefront radius, and $\eta(x) = 0.5 \ \mathrm{atan}\left(\frac{x}{x_0}\right)$ is the Gouy phase shift of the Gaussian beam near its waist.

The boundary conditions for the wave Eqs. (2) are set as follows. The front boundary condition is set to “scattering boundary”, with incident field given by Eq. (3):

$$\boldsymbol{e}_n \times (\nabla \times \boldsymbol{E}_q) - ik_q \boldsymbol{e}_n \times (\boldsymbol{E}_q \times \boldsymbol{e}_n) = -\boldsymbol{e}_n \times \left(\boldsymbol{E}_{q,inc} \times \left(ik_q(\boldsymbol{e}_n - \boldsymbol{e}_k)\right)\right) \exp\left[\left(-ik_q r\right)\right] \quad (4)$$

Here, e_n is the unit vector normal to the boundary surface, and e_k is the unit vector giving the incident wavevector direction. The back boundary condition, positioned at $x = 2x_0$, is also set to “scattering boundary”, with no incident field:

$$e_n \times (\nabla \times E_q) - ik_q e_n \times (E_q \times e_n) = 0 \quad (5)$$

The lateral boundaries, positioned at $y = 0$ and $y = 8w_0$, are set to “perfect electric conductor”:

$$e_n \times E_q = 0 \quad (6)$$

The 2D spatial mesh is set linear in both *x* and *y* directions, with a minimum step of 30 nm. Fig. 2 presents numerical results regarding the influence of pump-laser intensity, NL medium length, and focus position in the NL medium. Fig 2(a) indicates that intensity of TH radiation increases approximately linearly with third power of the pump intensity. Fig 2(b) indicates a maximum signal when the NL medium length *L*is equal to confocal parameter *b* (b=2x_0), followed by a decrease of the efficiency as the length of the NL medium increases.

Fig 2(c) indicates that the focus position is also an important factor in determining the TH signal: focusing the pump laser behind the NL medium leads to stronger signal as compared to focusing in center or in front of the NL medium.

These results were published in the paper "Theoretical and experimental study on geometry related phase-matching condition for third harmonic generation", U.P.B. Sci. Bull., Series A, Vol. 84 (2), 163-174 (2022)

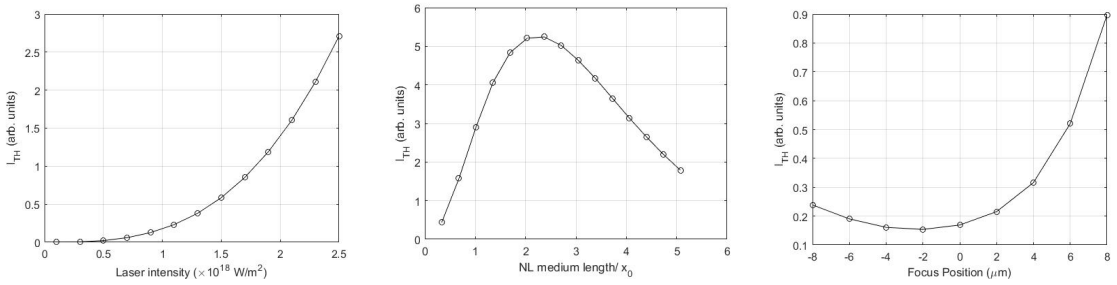

(a) (b) (c)

Fig. 2.Influence of different parameters on the intensity of third harmonic radiation: (a) pump intensity, (b) length of the NL medium, and (c) focus position in the NL medium.

We also modeled the harmonics generation by using ultrashort fs pulses. In this case, the non-linear time dependent wave equation is:

$$\nabla \times \left(\nabla \times \vec{E}\right) + \mu\sigma \frac{\partial \vec{E}}{\partial t} + \mu \frac{\partial}{\partial t}\left(\varepsilon_0 \frac{\partial \vec{E}}{\partial t} - \vec{P}\right) = 0 \quad (7)$$

where $\vec{P}$ has linear and nonlinear parts. The Fourier transform of the distorted output field corresponding to a 10 fs laser pulse (Fig. 3a) reveals the third harmonic radiation (Fig. 3b). These results were presented in the proceedings paper for the conference ATOM-N 2022.

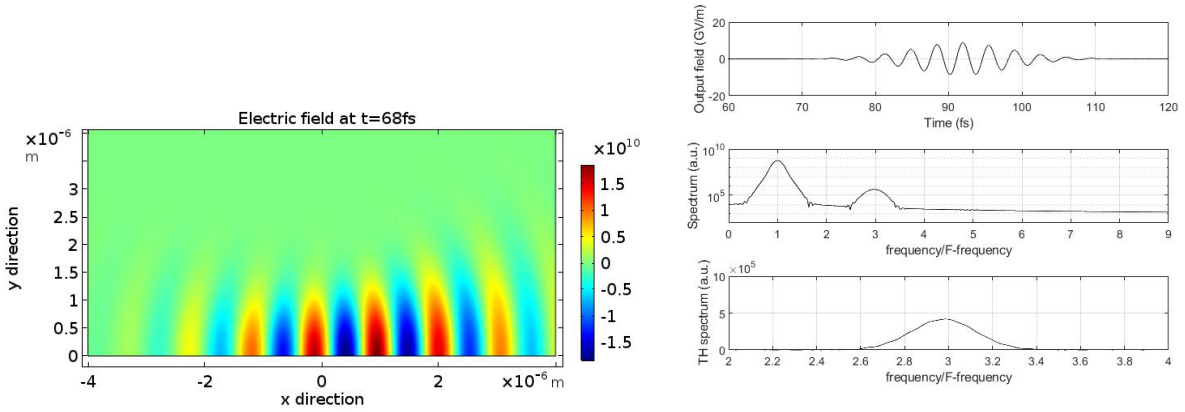

(a) (b)

Fig. 3. a) imulated spatial distribution of the electric field of the laser pulse at the moment 68 fs.(b) Numerical results on time dependence of the laser electric field at the output boundary (top), the corresponding spectrum calculated Fourier transform (middle) and spectrum of TH enabling calculation of TH intensity and width (bottom).
Fourier transform of the time dependent output signal demonstrates the presence of third harmonic signal along with the pump signal. The simulations were carried for two lengths of the NL medium: (a) $L=2x_0$, (b) $L=4x_0$.

Result 2: Experiments on efficiency of HHG on solid and gas targets

Experiments on generation and characterization of TH radiation were carried out with a "Brilliant" Q-switched Nd-YAG laser delivering linearly polarized infrared radiation at $\lambda_1 = 1064$ nm wavelength, $\tau_p = 4.5$ ns pulse duration at 10 Hz repetition rate, and *D*=6 mm beam diameter measured at $\frac{1}{e^2}$ of the Gaussian intensity profile. Laser pulses were focused on open air at ambient pressure P=760 Torr, by a *f*=3 cm focal-length lens, giving beam radius in focus $w_0 \cong 3.4\ \mu$ m and a peak intensity I_0 in the range of 10 to 140 TW cm^{-2}. These intensities are above air breakdown threshold, in accordance to previously reported threshold power $P_{bt} = 1$ MW.

The harmonics radiation emerging from the breakdown plasma is analyzed in the axial direction with a fiber-coupled spectrometer (Ocean Optics HR2000+, 0.1 nm spectral resolution) triggered by the Q-switch signal of the laser system. The collecting fiber-tip was set in axial position ~ 8 cm away from the lens focus. The dependence of TH radiation on F intensity is given in Fig. 4(a). To characterize the directionality of TH emission, we measured the TH beam diameter at ~8 cm away from the lens focus, as follows: we mounted the collecting fiber-tip of

the spectrometer on a 1D mechanical translation-stage of 10 μ m resolution and scanned it in transverse direction across the TH beam. The dependence of TH intensity on the position of the fiber-tip is presented in Fig. 4(b), revealing an approximate Gaussian profile of ~8 mm diameter, while F beam diameter at this position is 16 mm.

The influence of F polarization on the efficiency of THG was investigated by rotating a quarter waveplate in the range -45 to 45 degrees, with 5 degrees increment, to change the polarization state from circular to linear and back to circular (Fig. 4(c)). During plate rotation, the ellipticity ϵ was varied between -1 and 1, where $\epsilon = \pm 1$ correspond to circular polarization and $\epsilon = 0$ to linear polarization.

These results were published in the paper “Three-step model for third-harmonic generation in air by nanosecond lasers”, Journal of the Optical Society of America B-Optical Physics 38 (7), 2206-2214 (2021).

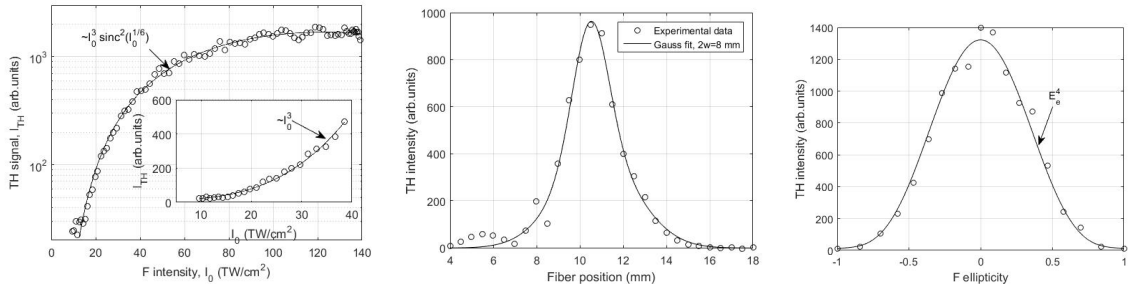

(a) (b) (c)

Fig. 4. (a) Experimental TH signal vs. F intensity. (b) TH signal recorded by translating radially the fiber-tip of the spectrometer. (c) TH signal vs. F ellipticity, ϵ . The solid line presents the fitting curve.

Result 3: Experimental study on the influence of kGy gamma doses on optical fibers used in collecting spectroscopic data.

Radiation effects in optical fibers can severely decrease the performance of these. Thus, we have evaluated the radiation induced changes in the optical transmission of commercially available optical fiber in order to evaluate their possible use for plasma diagnostics. Multimode optical fibers, for ultra-high vacuum (down to 10^{-10} Torr) and high temperature (up to 250^{o}C), were investigated. The optical transmission of optical fibers was measured, before and after gamma-rays irradiation, using a stabilized deuterium UV light source (200÷700nm) and an optical fiber spectrometer (Thorlabs) for wavelength range from 200 to 1000 nm. We studied the gamma radiation-induced effects on measured spectrum of the optical fiber output. Integration time of the spectral data was 143 μs.

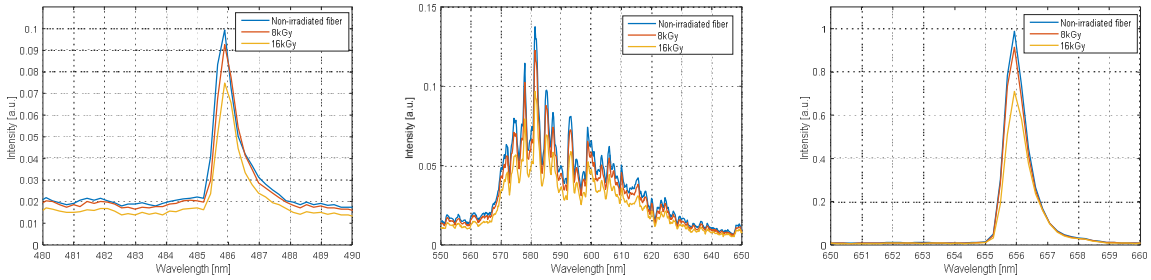

(a) (b) (c)

Figs. 5(a) The gamma radiation-induced effects on optical transmission spectrum in the 480-490 nm spectral band, **(b)** optical transmission spectrum in the 550-650 nm spectral band and **(c)** optical transmission spectrum in the 650-660 nm spectral band for a non-irradiated multimode optical fiber, an optical fiber irradiated by gamma-ray at 8 kGy and for an optical fiber exposed to gamma-ray irradiation at 16 kGy.

Two optical fibers with same characteristics were irradiated at 31^{o}C temperature, with a ^{60}Co gamma source. One fiber was irradiated with a dose of 8 kGy and the second optical fiber was exposed at a dose of 16 kGy. Figs. 5 present the gamma radiation-induced effects on optical fiber transmission spectrum. For better visibility we divided the spectral range into several spectral bands: 480-490 nm, 550-650 nm, 650-660 nm. As can be seen, in Figs. 5 the intensity decreases with the increase of the dose radiation. From the results presented in Fig. 5 one can see that, if gamma radiation is present, the degradation of the optical fibers occurs. In our case, the degradation manifests as photo-darkening, i.e. the decrease of the transmitted spectral intensity due to gamma irradiation. The transmitted spectra of the optical fiber have the same shape in the three cases presented here, but the spectrum intensity decreases in case of the irradiated fibers as compared to the non-irradiated fiber. Thus, the spectral intensity at 485.9 nm wavelength decreases by approximately 5% for the optical fiber irradiated at a dose of 8kGy, and by approximately 25% for the optical fiber exposed at a dose of 16kGy.

These results were presented in the proceedings paper for the conference ATOM-N 2022.

3. Deliverables in the last year related to the project:

- List of papers (journal or conference proceeding);

i. M. Stafe, “Three-step model for third-harmonic generation in air by nanosecond lasers”, JOURNAL OF THE OPTICAL SOCIETY OF AMERICA B-OPTICAL PHYSICS 38 (7), pp.2206-2214 (2021).

ii. Mihai STAFE, Constantin NEGUȚU, Georgiana C. VASILE, and Niculae N. PUȘCAȘ, "Theoretical and experimental study on geometry related phase-matching condition for third harmonic generation", U.P.B. Sci. Bull., Series A, Vol. 84, Iss. 2, 2022

iii.**http://www.physics.pub.ro/Departament_Fizica/Proiecte_cercetare/PHARDIPLAS/RO/index.html**

- List of talks of group members (title, conference or meeting, date);

submitted one paper for the Proceedings of an international conference (ATOM-N2022) to be held on August 2022. Paper title: *Third harmonics emission with nanosecond and femtosecond lasers in air. Gamma radiation effects on optical fibers,* Authors: Mihai Stafe, Georgiana C. Vasile, Răzvan Mihalcea, Constantin Daniel Neguț, Constantin Neguțu, Niculae N. Pușcaș.

- Other deliverables (patents, books etc.).

5. Further group activities (max. 1 page):

- Collaborations, education, outreach.
- ……

M. Stafe, N. N. Pușcaș,and C. Negutu collaborate with INFLPR- Magurele for studying theoretically and experimentally the target and particle acceleration by ultrashort high intensity laser pulsessuch those from CETAL facility. They will publish their results in ISI journals.

Mihai Stafe, Niculae N. Pușcaș, Georgiana Vasile and Constantin Negutu collaborate with INOE for the project: ”Memorie inovativă optică plasmonică rapidă pe bază de anizotropie foto-indusă (FOMAN)”; 2020-2022, University POLITEHNICA of Bucharest being a partner of the project.

The knowledge acquired during this project is used for teaching two courses in the IALA master program at University Politehnica of Bucharest: 'Laser and Optics' given by Prof. Dr. Niculae.N. Puscas, and 'High Power Lasers Engineering and applications' given by S.I. Dr. Mihai Stafe.

6. Research plan and goals for the next year

Research plan:

R1. Determination of main characteristics of optical fibres used near the target when exposed to UV, X and gamma radiation.

R2. Spectroscopic study on the properties of the generating plasmas as a function of laser properties

R3. Experimental study on properties of harmonics in relation to properties of generating plasma for plasma diagnosis.

The experimental work for this phase will be mainly carried at LILS and LOI facilities at UPB. Additional experiments on laser produced plasma will be carried at CETAL facility, while fiber irradiation with different gamma doses will be carried at IFA.

We will carry the experiments by using high power pulsed lasers: Q-switced laser (5 ns,1064 nm wavelength, 300 mJ pulse energy, focused intensity up to the order of 100 TW/cm^2)

and CPA mode-locked femtosecond laser (200 fs- 10 ps, 1030 nm wavelength, 1 mJ pulse energy, focused intensity up to the order of 1 PW/cm2). We will use gas and solid targets. Irradiation of the solid target will be carried at normal incidence (as in NTSA experiments) and 45 degrees incidence angle (as in usual HHG on solid targets experiments and the two-spot irradiation experiments proposed in section 3.1 “Requirements for laser beam configuration and parameters” of the TDRs).

We will analyze the dependence of the harmonics properties (i.e. intensity, polarization and divergence) on the properties of the driving laser pulses (intensity, polarization in focus) and of the laser-produced plasma (density and temperature). Spectroscopic measurements of the electromagnetic radiation originating in the plasma will be carried, and influence of the high frequency harmonics radiation on the optical-fibers transmission in the vicinity of the irradiated target will be evaluated.

We propose to publish 2 papers and present the results at one conference, 1 national patent application for the laser-plasma real-time diagnosis technology through the generated harmonics.